Particle Tracking Model Transport Process Verification: Diffusion Algorithm

by David B. King Jr. and Tahirih C. Lackey

PURPOSE: This Dredging Operations and Environmental Research Technical Note (DOER-TN) describes a new set of test cases developed to investigate the behavior of the diffusion algorithm contained within the Particle Tracking Model (PTM). The test cases were designed to examine different aspects of diffusion in isolation and in combination. The test cases needed to be complex enough to mimic real-world conditions but idealized enough to have analytical solutions for comparison. These test cases were developed to achieve two objectives: verification of the diffusion algorithm and the establishment of benchmark test cases to confirm that future model updates will not have inadvertently degraded capabilities. This technical note describes how the model outputs compare with analytical predictions.

INTRODUCTION: The PTM is a Lagrangian-based particle tracking model developed by the U.S. Army Corps of Engineers (USACE) Engineer Research and Development Center (ERDC) to efficiently track large numbers of particles as they move through complex flow fields. It allows the modeler to predict deposited and suspended sediment densities in space and time along with final particle fates (Demirbilek et al. 2004; Davies et al. 2005; McDonald et al. 2006; Lackey and McDonald 2007). Although a versatile model currently utilized in various coastal, estuarine, and riverine applications, PTM is specifically designed to predict the fate of material suspended during dredging and placement operations and to address the stability and fate of in-place sediment including dredged-material mounds, sediment caps, and contaminated sediment deposits. PTM models the physical processes of advection, diffusion, settling, deposition, burial, and resuspension, as appropriate for each parcel at each numerical time-step, to simulate the transport of a specified sediment distribution. Thus, required PTM inputs include a characterization of both the bed sediments and the tracked sediments. Instead of undertaking the impossible task of modeling every grain of sand, silt, and clay, sediment is discretized into *parcels*. Each parcel is representative of a specific mass of sediment. In aggregate, the specified sediment parcels preserve the overall size distribution and total mass of the sediment source. Along with position through time, each parcel is tagged with a variety of additional attributes such as mass, density, grain size, and suspension status.

PTM requires the input of hydrodynamics (i.e., water surface elevation and velocities), defined upon a bathymetry grid that is provided through an external model. This allows the modeler to perform multiple PTM runs to compare alternative sediment releases exposed to the same hydrodynamic conditions without the computational overhead of regenerating flow conditions for each hydrodynamic run. PTM operates within the Surface-water Modeling System (SMS), which provides effective visualization tools, making it useful for assessment of dredging practices and proposed dredging operations.

PTM DIFFUSION: PTM uses a random walk model to calculate the diffusion velocity. The horizontal component of the dispersive velocity (U_D) is assumed to be isotropic and is computed as

$$U_D = 2(\Pi - 0.5)\sqrt{\frac{6\varepsilon_D}{dt}} \text{ (m/s)} \tag{1}$$

where the horizontal eddy diffusivity (ε_D) is defined as

$$\varepsilon_D = K_{Et}hu^* \text{ (m}^2\text{/s)} \tag{2}$$

the shear velocity (u^*) as

$$u^* = \frac{U}{2.5\ln\left(\frac{11h}{k_s}\right)} \text{ (m/s)} \tag{3}$$

and the bottom roughness (k_s) as

$$k_s = 3 * D_{90} \text{ (m)} \tag{4}$$

In these equations, Π is a random number uniformly distributed between 0 and 1, U is the free stream flow velocity (m/s), K_{Et} is the horizontal turbulent diffusion scalar, h is the flow depth (m), and D_{90} is the 90th percentile sediment diameter (i.e., 90% of the sediment grains, by weight, have diameters smaller than this value) (m). These equations are all discussed in further detail in MacDonald et al. (2006) and Lackey and MacDonald (2007).

The vertical component of the diffusion velocity (W_D) is computed similarly as

$$W_D = 2(\Pi - 0.5)\sqrt{\frac{6\varepsilon_v}{dt}} \text{ (m/s)} \tag{5}$$

Based upon Fischer et al. (1979), PTM's vertical eddy diffusivity (ε_V) algorithm has been updated from that given in MacDonald et al. (2006) to

$$\varepsilon_V = \frac{h}{2}K_{Ev}U\left[\frac{z(h-z)^2}{h^3}\right] \text{ (m}^2\text{/s)} \tag{6}$$

2

where K_{Ev} is the vertical turbulent diffusion scalar and z is the particle's vertical position in the water column (m). It is seen that the vertical eddy diffusivity has a parabolic dependence upon the vertical location, and at mid-depth, Eq. 6 reduces to

$$\varepsilon_V = K_{Ev}hU/16 \text{ (m}^2\text{/s)} \tag{7}$$

PTM allows the modeler to scale the turbulence levels in the model by accepting user-defined values for K_{Et} and K_{Ev}. One of three turbulence conditions ($\varepsilon_D = 0$, $\varepsilon_V = 0$, or $\varepsilon_D = \varepsilon_V$) was used in each of the tests in this report. The third condition was satisfied by releasing neutrally dense parcels at mid-depth and setting:

$$K_{Ev} = \frac{16\varepsilon_V}{hU} = \frac{16K_{Et}u^*}{U} \tag{8}$$

METHODS: The series of test cases described in this report were designed to examine diffusion along each axis independently and jointly. Tests 1–7 employed a steady one-dimensional (1D) flow field that was aligned with the axis of the channel (i.e., the x-direction). Tests 1–3 looked at diffusion in the x- (down-channel), y- (cross-channel), and z- (vertical) directions, respectively, in isolation. Tests 4–6 examined pair-wise diffusion in the x- and y-, the x- and z-, and the y- and z- directions, respectively. Additionally, Test 6 looked at y- and z-directed diffusion using two different parcel release protocols (Tests 6a and 6b). Test 7 examined diffusion occurring along all three axes simultaneously. Tests 8 and 9 also examined diffusion in all three axis directions. Test 8 used an unsteady 1D flow (a combined sinusoidal and steady flow that resembled aspects of a tidal flow in a river). Test 9 employed a steady two-dimensional (2D) flow field (rotational flow about a central point that resembled aspects of a vortex flow). Table 1 lists the conditions for each test.

For all the tests, PTM released neutrally buoyant parcels at mid-depth in a flat basin. Flows experienced zero friction (slip conditions) at all side and bottom boundaries. That is, flows did not include logarithmic boundary layer profiles. In addition, the tests were designed such that parcels remained well away from side and bottom boundaries at all times.

Each of the tests employed one of four types of parcel release protocols: instantaneous cross-flow line source release, instantaneous along-flow line source release, instantaneous point source release, or continuous point source release. Examples of these four types of releases are shown in plan view in Figure 1, panels A–D, respectively. Each of these examples shows the release point as a black line or point centered near the left-hand (upstream) end of the panel and a cloud of red parcels at a time after release or after initial release. The clouds of parcels have expanded over time by diffusion as they have been advected downstream (i.e., in the x-direction) from the release site.

3

Table 1. Test cases.					
Test Name	Axes of Diffusion	Source Type	Horizontal Diffusion	Vertical Diffusion	Flow Type
1	x	ICfLS	On	Off	1D Steady
2	y	IAfLS	On	Off	1D Steady
3	z	IPS	Off	On	1D Steady
4	x,y	IPS	On	Off	1D Steady
5	x,z	ICfLS	On	On	1D Steady
6a	y,z	IAfLS	On	On	1D Steady
6b	y,z	CPS	On	On	1D Steady
7	x,y,z	IPS	On	On	1D Steady
8	x,y,z	IPS	On	On	1D Sinusoidal
9	x,y,z	IPS	On	On	2D Steady

IPS = Instantaneous Point Source (Figure 1-C)
ICfLS = Instantaneous Cross-flow Line Source (Figure 1-A)
IAfLS = Instantaneous Along-flow Line Source (Figure 1-B)
CPS = Continuous Point Source (Figure 1D)

RESULTS

Test 1. This test examined PTM diffusion in the *x*-direction in isolation that is generated by a 1D steady flow. The analytical solution of the 1D diffusion equation (Fischer et al. 1979) is

$$C(x,t) = \left[\frac{M}{\sqrt{4\pi\varepsilon_D t}} \right] \exp\left[\frac{-(x-Ut)^2}{4\varepsilon_D t} \right] \text{(kg/m)} \tag{9}$$

where $C(x,t)$ is the 1D particle concentration (kg/m), M is the total mass of particles released (kg), and t is time (s).

This concentration can be converted to a density (kg/m^3) by assuming a constant distribution of this concentration that is 1 m high by 1 m wide. The analytical standard deviation (σ) for this Gaussian distribution is

$$\sigma = \sqrt{2\varepsilon_D t} \text{ (m)} \tag{10}$$

The location of the centroid (= Ut) is a function of time in the *x*-direction. Its position remains unchanged at its midchannel location in *y* and at its mid-depth location in *z*.

For this PTM run, parcels were released instantaneously along a cross-flow line (Figure 1A). This type of release eliminated the effects of diffusion in the cross-flow (*y*) direction by making it constant so long as the parcel sampling scheme stayed well clear of the ends of the line. Parcels experienced no vertical motion because gravity was nullified by creating neutrally dense particles, and vertical diffusion was eliminated by setting $K_{Ev} = 0$.
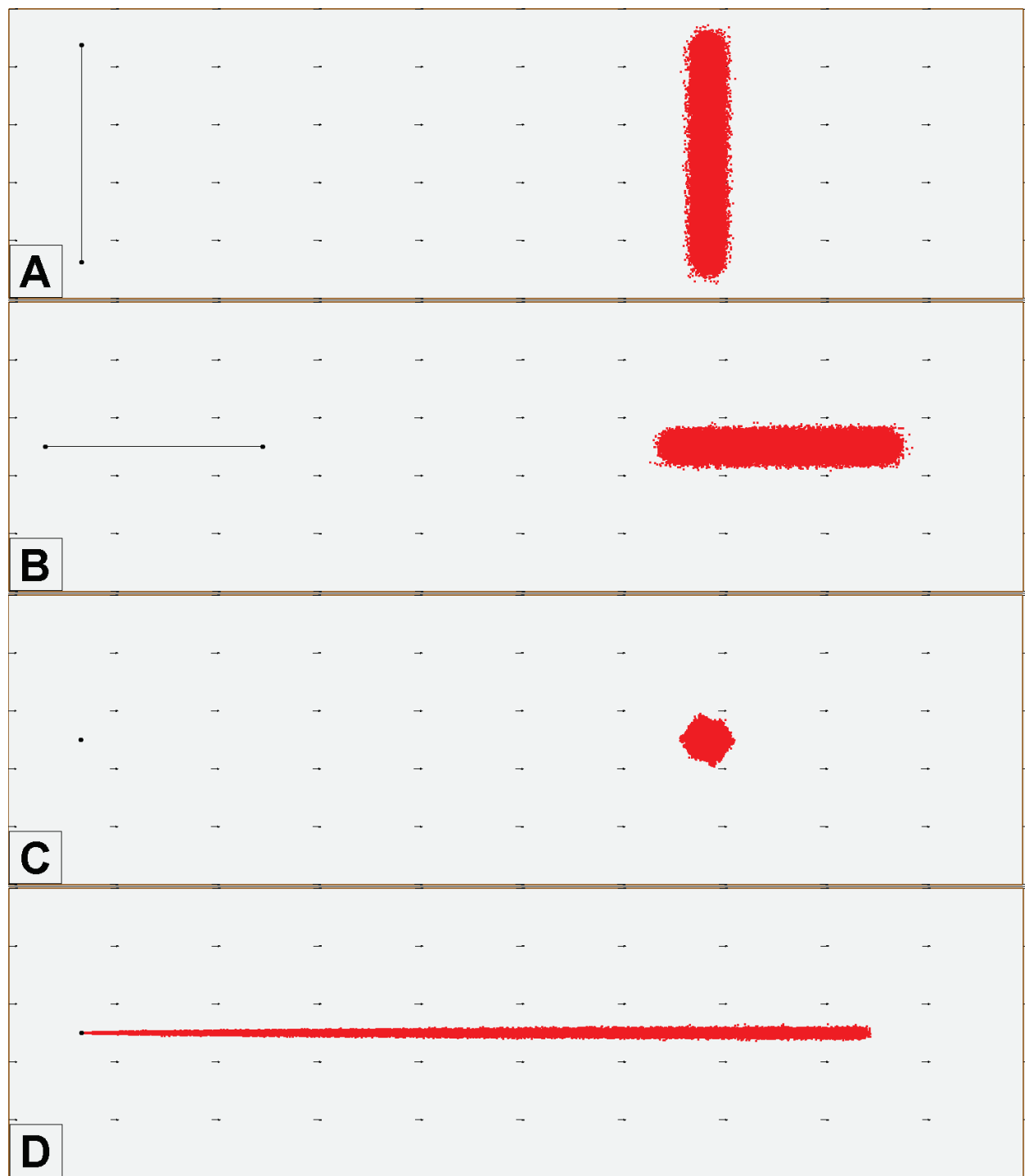
4

Figure 1.   Examples of four types of parcel release protocols. See text for explanation.

The effects of along-flow directed diffusion were measured by examining the distribution of parcels contained within the black (solid line) rectangular sampling region shown in Figure 2A. The cross-flow limits on the sampling region were set by having them be $> 5\sigma$ from the centroid-translated ends of the release line. In the along-flow direction, the sampling region was centered about the analytical centroid of the distribution (i.e., Ut), and the width was set at $\pm 4.59\sigma$. The

sampling region was then divided into 51 bins, each extending the width of the sampling region in the cross-flow direction and being 0.18σ wide in the along-flow direction. Figure 2B shows a blowup of the area of Figure 2A within the dashed green box and includes a section of the centroid-translated release line (blue line) and the ends of the 51 sample bins (black lines).

This binning procedure was applied in a similar way for all the tests. By trial-and-error, it was determined that this binning methodology provided an appropriate resolution of underlying distribution without overly-smoothing the data. The number of parcels within each bin was counted, and the sum was converted to a concentration. A comparison of the PTM parcel distribution with the expected Gaussian distribution is shown in Figure 3, panel A.
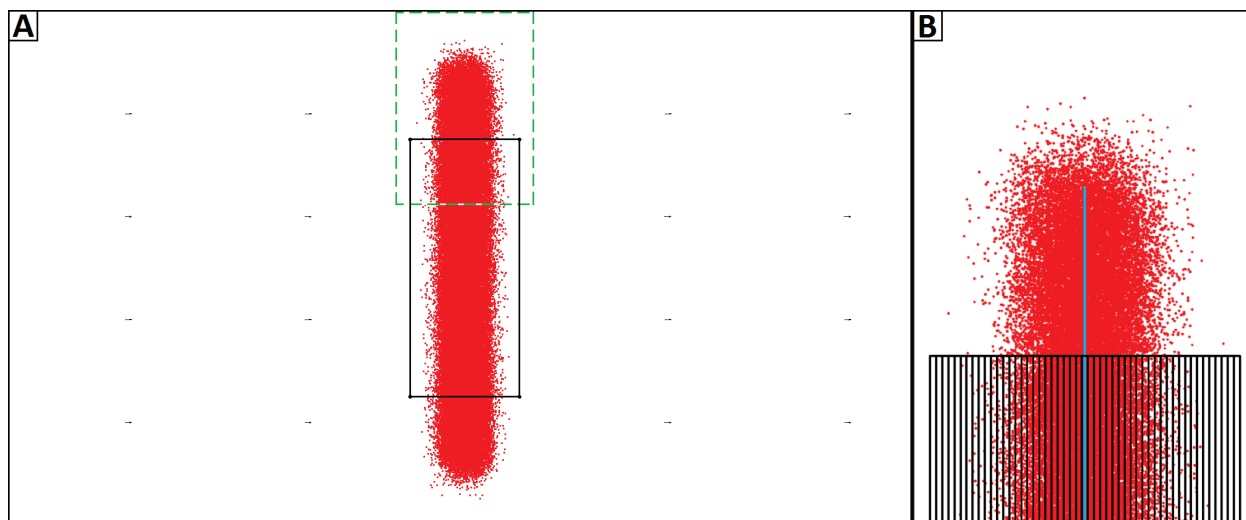

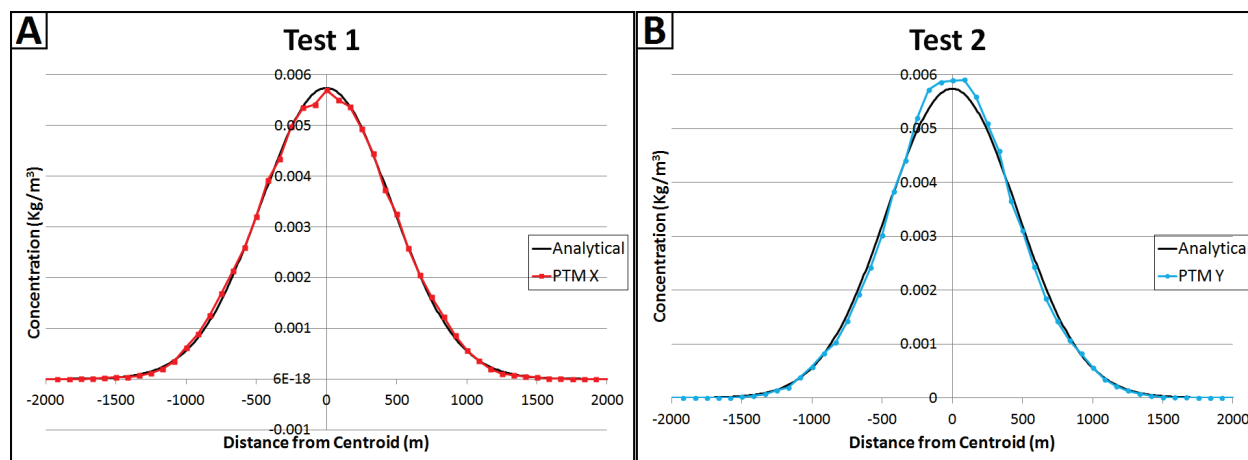Figure 2.   Sampling region and binning scheme. See text for discussion.

Figure 3.   Comparison results for Tests 1 and 2.

Comparisons of the results for all the tests are shown in Table 2. In this table, the individual tests are in the different columns. A comparison of *x*-directed diffusion created by PTM with that predicted by the analytical solution is given in the upper block of rows, *y*-directed diffusion in

6

the center block and *z*-directed diffusion in the lower block. "St Dev Ratio" (standard deviation) is the PTM calculated values divided by the analytical values. The analytical values for "Skewness" and "Kurtosis" are zero. "Max Ht Ratio" is a ratio of the maximum heights of the two distribution curves (PTM/Analytical). "Area Ratio" is a comparison of the areas under the two distribution curves (PTM/Analytical), and "Corr Coef" (correlation coefficient) is a statistical, pair-wise comparison of the values comprising the two curves.

Table 2. Comparison statistics between measured and analytical results.											
	Test #	1	2	3	4	5	6a	6b	7	8	9
X	# of samples	66,640			37,261	24,576			47,120	100,000	15,843
	St Dev Ratio	1.00092			1.05231	1.00141			1.01248	0.95754	0.97175
	Skewness	-0.00064			0.00787	-0.00509			0.00501	0.00084	-0.00896
	Kurtosis	-0.12560			-0.01067	-0.20061			-0.06432	0.03118	0.13095
	Max Ht Ratio	0.99299			1.00293	0.98751			1.02431	1.10306	1.08147
	Area Ratio	0.99951			1.00000	0.99997			0.98688	1.00000	0.99545
	Corr Coef	0.99957			0.99984	0.99958			0.99921	0.99780	0.99464
Y	# of samples		66,615		38,290		24,741	3,872	47,104	100,000	16,410
	St Dev Ratio		0.96771		1.02275		0.95071	1.00792	0.99841	0.95340	0.98120
	Skewness		0.00154		-0.00018		-0.00173	0.04556	-0.00167	0.00072	0.09682
	Kurtosis		-0.01725		-0.23361		0.13691	0.15142	-0.12758	-0.09190	0.06496
	Max Ht Ratio		1.02892		0.96449		0.96966	0.98702	0.98814	1.01129	1.06047
	Area Ratio		0.99913		1.00000		0.93020	0.96295	0.98655	1.00000	1.03108
	Corr Coef		0.99885		0.99949		0.99463	0.99395	0.99944	0.99942	0.99771
z	# of samples			100,000		25,028	26,634	3,786	45,081	100,000	16,363
	St Dev Ratio			0.97025		1.05216	1.06527	0.99666	0.96051	0.91991	0.91293
	Skewness			0.00049		0.00106	-0.00657	-0.02119	-0.00163	0.00061	0.02048
	Kurtosis			-0.11943		-0.00570	0.03067	-0.02953	0.04459	-0.11803	-0.36331
	Max Ht Ratio			1.02159		0.96718	0.98798	1.00167	1.02985	1.10069	1.03160
	Area Ratio			1.00000		0.99997	1.00138	0.95219	0.94418	1.00000	1.02812
	Corr Coef			0.99969		0.99933	0.99897	0.99541	0.99805	0.99774	0.99773

Test 2. This test examined PTM diffusion in the *y*-direction in isolation that is generated by a 1D steady flow. The influence of diffusion in the *x*-direction was eliminated by making it constant in a way analogous to that described for Test 1. The instantaneous along-flow line source type of parcel release is shown in Figure 1B. Figure 3B compares the model output with the analytical solution.

Test 3. This test examined PTM diffusion in the *z*-direction in isolation that is generated by a 1D steady flow. The influence of diffusion in the *x*- and *y*-directions were negated by setting K_{Et} = 0. Parcels were released as an instantaneous point source. At a later time, they would still appear as a point in plan view (rather than as a cloud as shown in Figure 1C). In side view, the distribution of parcels would appear as a vertical line (overlapping row of dots) centered at mid-depth that increases in length as it is advected downstream. Figure 4A compares the model output with the analytical solution.
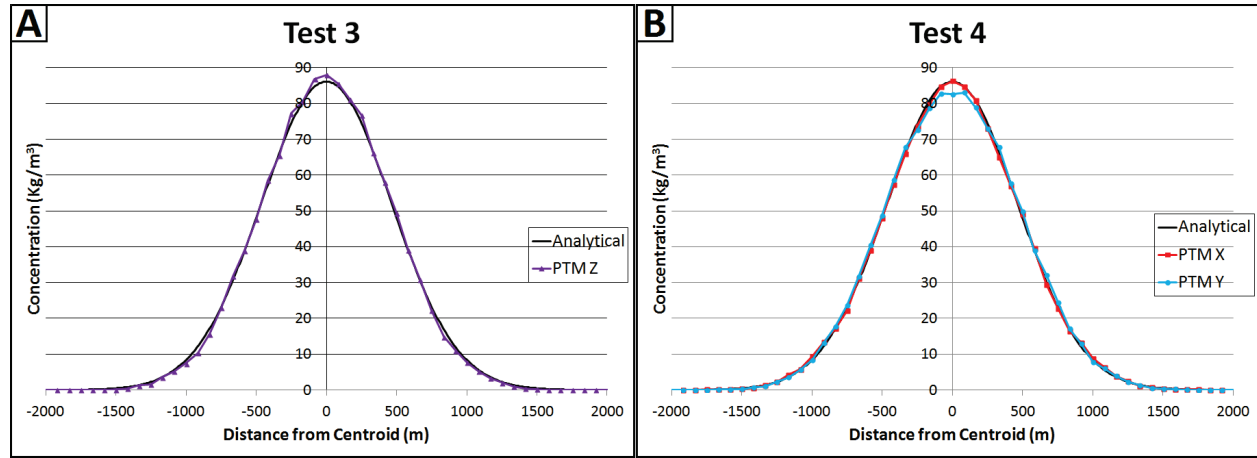
Figure 4.   Comparison results for Tests 3 and 4.

Test 4. This test examined PTM diffusion in the *x*- and *y*- directions generated by a 1D steady flow. Vertical diffusion is turned off. Parcels were released as an instantaneous point source as shown in Figure 1C. The analytical concentration per unit area (Fischer et al. 1979) is

$$C(x,y,t) = \frac{M}{4\pi\varepsilon_D t} \exp\left\{\frac{-[x-U_C t]^2 - y^2}{4\varepsilon_D t}\right\} \text{ (kg/m}^2\text{)} \tag{11}$$

The standard deviation of this distribution is also given by Equation 10. Figure 4B compares the model output for this test with the analytical solution.

Test 5. This test examined PTM diffusion in the *x*- and *z*-directions generated by a 1D steady flow. Parcels were released as an instantaneous cross-flow line source (Figure 1A), and cross-flow diffusion was eliminated as described for Test 1. However, for this test, the vertical diffusion was turned on. Equation 11 describes the analytical concentration (with the *y* variable replaced by the *z* variable). Figure 5A compares the model output with the analytical solution.

Test 6a. This test examined PTM diffusion in the *y*- and *z*-directions using an along-flow instantaneous line source release (Figure 1B) generated by a 1D steady flow. This test is similar to Test 2 with the vertical diffusion turned on. Figure 5B compares the model output with the analytical solution.

8

Test 6b. This test provided an alternative release methodology to examine PTM diffusion in the *y*- and *z*-directions from that presented in Test 6a. This test examined vertical and horizontal cross-flow transects through a plume (Figure 1D). The steady state analytical solution, from Fischer et al. (1979),

$$C(x,y,z) = \frac{M_s}{4\pi\varepsilon_D x} \exp\left(-\frac{(y^2+z^2)U_c}{4\varepsilon_D x}\right) \text{ (kg/m}^2\text{)} \tag{12}$$
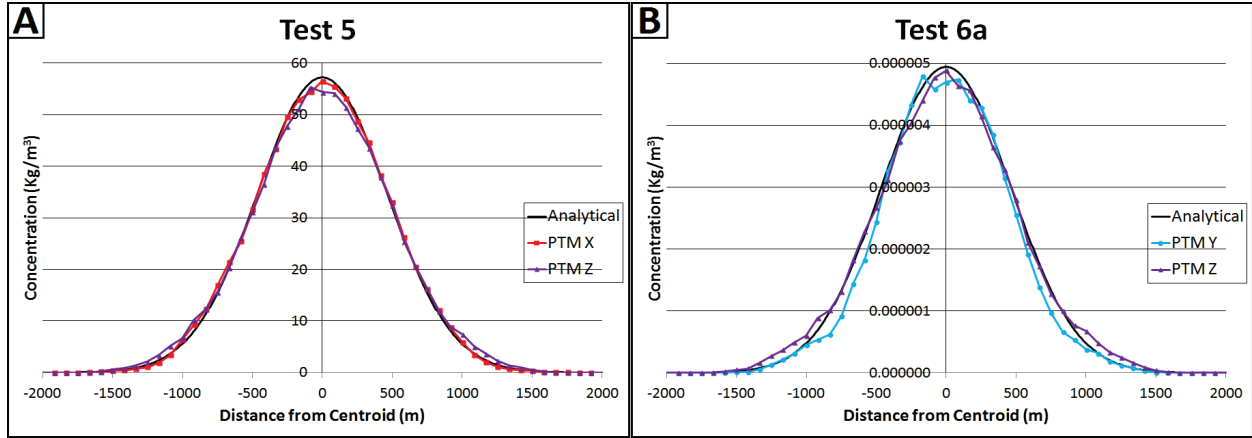

Figure 5. Comparison results for Tests 5 and 6a.

is valid provided that the transects are sufficiently far upstream from the head of the plume. In this equation, M_s is the mass rate of parcel release. The standard deviation for this solution is

$$\sigma = \sqrt{2\varepsilon_D x/U} \text{ (m)} \tag{13}$$

For this test, the PTM output was analyzed at a position > 5 σ upstream of the head of the plume (defined as the *Ut* position, with t_0 being the time of first release). Figure 6A compares the model output with the analytical solution. The increased level of noise in the PTM solutions for this case is largely due to the smaller numbers of parcels within the sampled region (Table 2).

Test 7. This test examined PTM diffusion in the *x*-, *y*-, and *z*-directions generated by a 1D steady flow with an instantaneous point source release (Figure 1-C). The analytical solution (from Fischer et al. 1979) is given as

$$C(x,y,z,t) = \left[\frac{M}{(4\pi\varepsilon_D t)^{3/2}}\right]\exp\left[\frac{-(x-Ut)^2 - y^2 - z^2}{4\varepsilon_D t}\right] \text{ (kg/m}^3\text{)} \tag{14}$$

The standard deviation of this distribution is again given by Equation 10. Figure 6B compares the model output with the analytical solution.
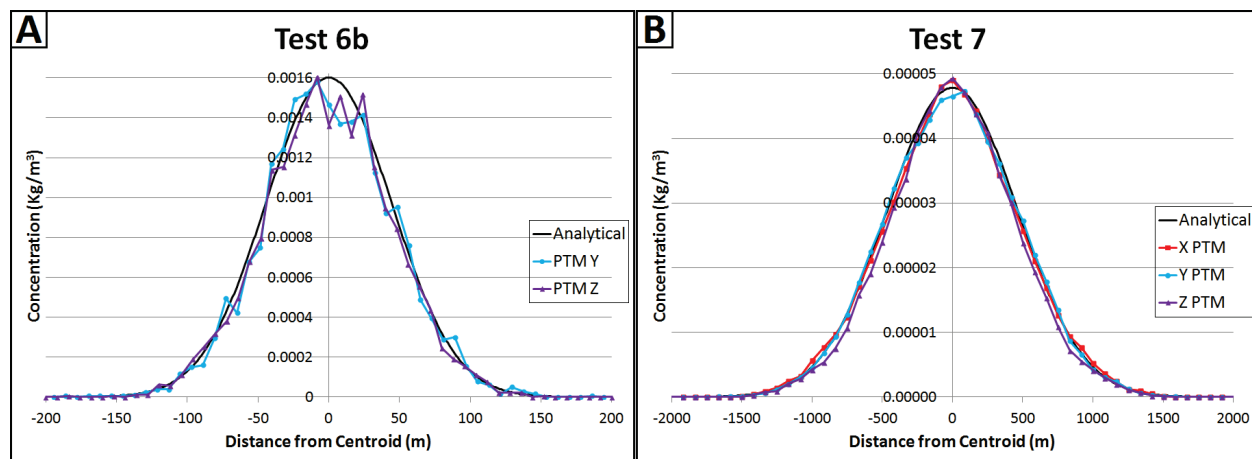
Figure 6.   Comparison results for Tests 6b and 7.

Test 8. This test examined PTM diffusion in the *x*-, *y*-, and *z*-directions generated by a 1D unsteady flow. The parcels were released as an instantaneous point source (Figure 1C). The flow was primarily sinusoidal, but the addition of a small steady (*x*-directed) component meant that at the end of each cycle, the centroid was advected farther downstream. For this test, the eddy diffusivity is no longer a constant but changes with each model time-step because of the changing velocity, as seen in Equations 2 and 6. To calculate the analytical concentration (Equation 14) and standard deviation (Equation 10) for this comparison, an root-mean-square value of the velocity was used to calculate the eddy diffusivity. For convenience, the time picked for a comparison was at the end of a flow cycle. Figure 7A compares the model output with the analytical solution.
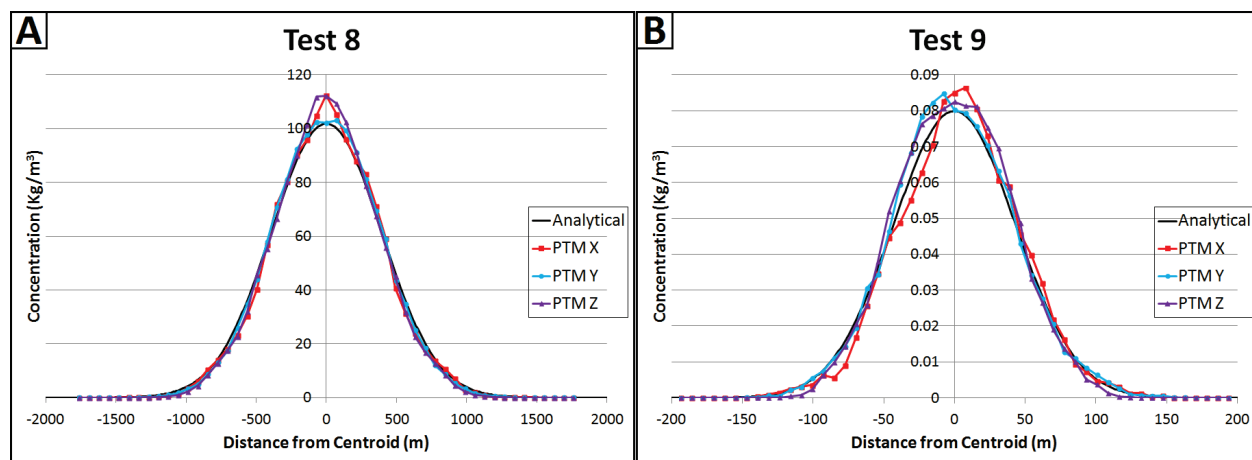

Figure 7.   Comparison results for Tests 8 and 9.

Test 9. This test examined PTM diffusion in the *x*-, *y*-, and *z*-directions generated by a 2D steady flow. The horizontal flow field rotated about a central point, mimicking solid-body rotation. Parcels were released as an instantaneous point source at a position away from the center of the flow and analyzed at the end of one revolution (Figure 8). A graphical comparison of the PTM distributions with the analytical solution is shown in Figure 7B.

10

SUMMARY AND CONCLUSIONS: A series of tests were conducted to verify the proper functioning of the diffusion algorithm in PTM. These tests examined diffusion along all three axes independently and jointly. Most tests used a 1D steady flow field, but some used more complex flows, including 1D unsteady flow and 2D steady flow. All tests compared the distribution of particles generated by PTM with their analytical solutions. The results of the comparisons are provided in Table 2. All of the types of comparisons, including the correlation coefficients, show strong agreement between the PTM particle distributions and the analytical distributions. Therefore, for all the test cases examined, this research found that the PTM diffusion algorithm behaves as expected.
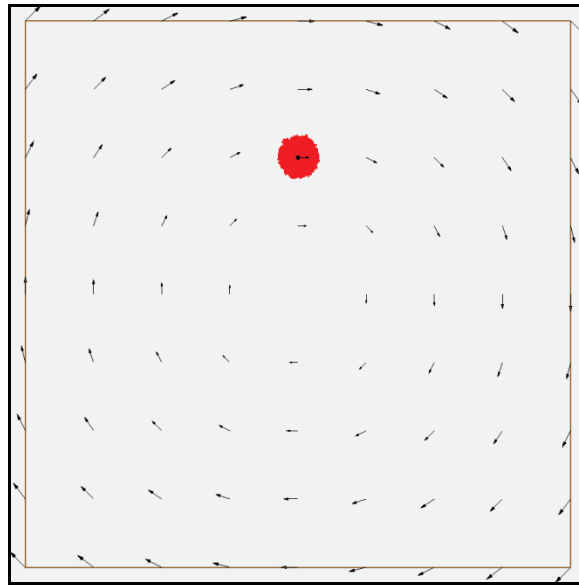
Figure 8.   2D flow grid and parcel positions after one complete flowfield revolution for Test 9.

King, D., and Lackey, T. 2015. Particle Tracking Model transport process verification: Diffusion algorithm. ERDC TN-DOER-D18. Vicksburg, MS: U.S. Army Engineer Research and Development Center. *http://el.erdc.usace.army.mil/dots/doer/pubs.cfm?Topic=TechNote&Code=doer*

REFERENCES

Davies, M. E., N. J. MacDonald, Z. Demirbilek, J. S. Smith, A. K. Zundel, and R. D. Jones. 2005. *Particle Tracking Model (PTM) in the SMS: II. An overview of features and capabilities*. Dredging Operations and Engineering Research Technical Notes Collection. ERDC TN-DOER-D5. Vicksburg, MS: U.S. Army Engineer Research and Development Center.

Demirbilek, Z., J. S. Smith, A. K. Zundel, R. D. Jones, N. J. MacDonald, and M. E. Davies. 2004. *Particle Tracking Model (PTM) in the SMS: I. Graphical interface*. Dredging Operations and Engineering Research Technical Notes Collection. ERDC TN-DOER-D4. Vicksburg, MS: U.S. Army Engineer Research and Development Center.

Fischer, H. B., E. J. List, R. C. Y. Kohl, J. Imberger, and N. H. Brooks. 1979. *Mixing in inland and coastal waters*. New York: Academic Press.

Lackey, T. C., and N. J. MacDonald. 2007. The Particle Tracking Model description and processes*. In *Proceedings, XVIII World Dredging Congress 2007, WEDA, Lake Buena Vista, Florida, USA*.

MacDonald, N. J., M. H. Davies, A. K. Zundel, J. D. Howlett, Z. Demirbilek, J. Z. Gailani, T. C. Lackey, and S. J. Smith. 2006. *PTM: Particle Tracking Model; Report 1: Model theory, implementation, and example applications*. ERDC/CHL TR-06-02. Vicksburg, MS: U.S. Army Engineer Research and Development Center.

ACRONYMS AND ABBREVIATIONS

Term	Definition
CHL	Coastal and Hydraulics Laboratory
DOER	Dredging Operations and Environmental Research
DOER-TN	Dredging Operations and Environmental Research Technical Note
ERDC	Engineer Research and Development Center
PTM	Particle Tracking Model
SMS	Surface-water Modeling System
USACE	U.S. Army Corps of Engineers